The EMBO Journal vol.13 no.21 pp.5075–5085, 1994

Adenovirus replication and transcription sites are spatially separated in the nucleus of infected cells

Ana Pombo[1], João Ferreira, Eileen Bridge[2] and Maria Carmo-Fonseca[3]

Institute of Histology and Embryology, Faculty of Medicine, University of Lisbon, 1699 Lisboa Codex, Portugal and [2]Department of Medical Genetics, Box 589, Biomedical Center, Uppsala University, S-75123 Uppsala, Sweden
[1]Present address: Sir William Dunn School of Pathology, South Parks Road, Oxford OX1 3RE, UK
[3]Corresponding author

Communicated by A.Lamond

We have visualized the intranuclear topography of adenovirus replication and transcription in infected HeLa cells. The results show that viral DNA replication occurs in multiple foci that are highly organized in the nucleoplasm. Pulse–chase experiments indicate that newly synthesized viral double-stranded DNA molecules are displaced from the replication foci and spread throughout the nucleoplasm, while the single-stranded DNA replication intermediates accumulate in adjacent sites. Double-labelling experiments and confocal microscopy show that replication occurs in foci localized at the periphery of the sites where single-stranded DNA accumulates. The simultaneous visualization of viral replication and transcription reveals that the sites of transcription are predominantly separated from the sites of replication. Transcription is detected adjacent to the replication foci and extends around the sites of single-stranded DNA accumulation. These data indicate that newly synthesized double-stranded DNA molecules are displaced from the replication foci and spread in the surrounding nucleoplasm, where they are used as templates for transcription. Splicing snRNPs are shown to co-localize with the sites of transcription and to be excluded from the sites of replication. This provides evidence that splicing of viral RNAs occurs co-transcriptionally and that the sites of viral DNA replication are spatially distinct from the sites of RNA transcription and processing.
Key words: adenovirus 2/nuclear localization/transcription/replication

Introduction

The nucleus of eukaryotic cells is a highly organized organelle that performs several essential functions such as DNA replication and RNA transcription, processing and transport, each involving a multitude of complex reactions that are precisely controlled and regulated. Although cell biologists have long thought that the nucleus must be highly structured, the mechanisms responsible for nuclear organization are just beginning to be unravelled. The finding that many nuclear components and activities are localized in discrete subnuclear domains rather than being diffusely distributed in the nucleoplasm strongly suggests that there is an underlying structure that may determine the functional organization of the nucleus (for recent reviews see Berezney, 1991; Jackson, 1991; VanDriel *et al.*, 1991; Xing *et al.*, 1993; Spector, 1993).

Recent data from several laboratories have shown that introducing new active sites of replication and transcription in mammalian cells can cause important structural rearrangements in the nucleus (Martin *et al.*, 1987; Walton *et al.*, 1989; Bosher *et al.*, 1992; Bridge *et al.*, 1993; Jiménez-Garcia and Spector, 1993; Phelan *et al.*, 1993; Puvion-Dutilleul and Christensen, 1993). Most of these studies have relied upon infection of cells with viruses which subvert the host cellular mechanisms in order to replicate and express their own genomes. Adenoviruses in particular have long been considered an invaluable model for understanding the mechanisms of mRNA transcription and processing in mammalian cells (reviewed by Ziff, 1980; Flint, 1986), as well as the roles played by specific cell regulatory proteins (reviewed by Moran, 1993). Recently, adenoviruses have further acquired special interest as one of the most effective viral vehicles for gene therapy (see Mulligan, 1993). While the molecular events involved in adenovirus DNA replication and RNA transcription have been extensively studied, the mechanisms responsible for interaction of the viral genomes with the host nuclear structure remain largely unknown.

Adenovirus type 2 (Ad2) and the very similar Ad5 are members of the group C human adenoviruses and consist of an icosahedral particle with a double-stranded genomic DNA and 11–15 structural proteins (Horwitz, 1990). Ad2 causes a productive infection of HeLa cells that proceeds through an infectious cycle of ~36h. This cycle is conventionally divided into early and late stages, separated by the onset of viral DNA replication at ~8 h post-infection (see Philipson *et al.*, 1975). Adenoviruses enter the host cells by receptor-mediated endocytosis, penetrate the cytosol from endosomes and deliver their DNA genome into the nucleus (Greber *et al.*, 1993). Upon entry in the nucleus, transcription of the viral genome starts immediately and by 3–5 h post-infection ~15% of the mRNA in the cytoplasm is virus-encoded (Philipson *et al.*, 1975). The viral mRNAs transcribed during this early phase correspond to the expression of only 20–40% of the viral genome and direct the synthesis of a small number of proteins which interact with specific cellular proteins that normally act to restrict cell growth (reviewed by Moran, 1993), as well as proteins required for viral DNA replication (see Challberg and Kelly, 1989; Horwitz, 1990). Therefore, the early phase of infection appears to be primarily directed towards priming the infected cell for viral DNA replication. Following initiation of viral DNA replication (at 6–8 h post-infection), almost all the

remaining viral genomic information is expressed, yielding prodigious quantities of the structural proteins that will eventually constitute new virus particles (Philipson *et al.*, 1975; Flint, 1986).

The Ad genome is a double-stranded linear DNA with ~35 000 bp. The 5′ end of each strand is covalently attached to a virus-encoded protein called the terminal protein (TP), and the nucleotide sequences at the extreme ends of the DNA are identical (for a review see Horwitz, 1990). Ad DNA replication requires three virus-encoded proteins: the TP, the Ad DNA polymerase (Ad pol) and the single-stranded DNA binding protein (termed 72K or DBP); in addition, several cellular proteins are necessary, including two transcription factors (NF-I/CTF and NF-III/OTF-1) and a topoisomerase I activity (reviewed by Challberg and Kelly, 1989; Horwitz, 1990). The Ad pol has physical and biochemical properties distinct from other known eukaryotic DNA polymerases, namely it is relatively inactive with RNA primers and it is less sensitive to aphidicolin (Kwant and van der Vliet, 1980). Ad DNA replication is initiated at either terminus of the double-strand by a protein priming mechanism that involves the terminal protein and results in the establishment of a replication fork that moves from one end of the genome to the other. At each replication fork only one of the two parental DNA strands is replicated, producing a daughter duplex and a displaced single-strand (ssDNA). It is only in a second stage of DNA replication that the displaced single-strand serves as a template for synthesis of a complementary strand (Challberg and Kelly, 1989).

In contrast with replication, Ad makes use of the cellular RNA polymerases II and III to transcribe its DNA. RNA polymerase II transcribes the majority of the viral genome, whereas RNA polymerase III transcribes two small non-coding RNAs called virus-associated RNAs (VA RNAI and VA RNAII) (Ziff, 1980; Mathews and Shenk, 1991). To maximize its small genome, adenovirus has evolved complex transcription units in which the primary transcripts are processed in different ways to produce different end products. The processing and maturation of viral mRNAs is carried out by the host cellular machinery and involves capping, polyadenylation, methylation and splicing (Darnell, 1982; Tooze, 1982; Ziff, 1980; Sharp, 1984).

In this work we have simultaneously visualized the sites of Ad replication and transcription in the nucleus of infected HeLa cells. We find that viral DNA replication occurs in foci localized at the surface of goblet-shaped structures that represent sites of viral ssDNA accumulation, whereas transcription is predominantly detected around these structures. Pulse–chase experiments indicate that as new DNA molecules are synthesized in the replication foci, the pre-existing ones are displaced in a vectorial way. The data indicate that single-stranded replication intermediates are displaced into adjacent accumulation sites whereas the double-stranded DNA molecules spread to the surrounding nucleoplasm where they serve as templates for RNA synthesis. Splicing snRNPs are shown to redistribute and to become concentrated at the sites of viral transcription, suggesting that splicing of viral mRNAs is co-transcriptional.

Results

Visualization of adenovirus DNA and RNA

Both uninfected and infected HeLa cells were hybridized *in situ* under non-denaturing conditions using a biotinylated Ad2 genomic probe. At 18 h post-infection the cells showed a strong hybridization signal (Figure 1a and d), whereas uninfected cells were not labelled (Figure 1i). However, not all infected cells revealed similar labelling patterns, reflecting the asynchrony of the viral infection. The hybridization signals observed at this time post-infection ranged from tiny intranuclear foci to an overall staining of both the nucleus and the cytoplasm (Figure 1a). Time-course experiments indicated that at 7–14 h post-infection the hybridization signal in the majority of cells was restricted to discrete nuclear foci or dots, whereas between 14–24 h post-infection there was a progressively higher percentage of cells labelled intensely both in the nucleus and in the cytoplasm (data not shown). Within the nucleus, the labelling was mostly concentrated in discrete pleomorphic domains which correspond to structures labelled by antibodies directed to the viral protein DBP (Figure 1d and g and other data not shown).

Since Ad2 DNA replication induces the formation of single-stranded DNA (ssDNA) intermediates that accumulate in the nucleus of infected cells (see Challberg and Kelly, 1989), the intranuclear labelling observed by *in situ* hybridization under non-denaturing conditions using a genomic probe depicts the localization of both viral RNA and ssDNA. Thus, in order to distinguish between Ad2 RNA and ssDNA we performed nuclease digestions with DNase I and RNase A, respectively, before hybridization. Following digestion of infected cells with RNase A, the hybridization signal was completely abolished from the cytoplasm, demonstrating that the cytoplasmic staining represents viral RNA (Figure 1b and e). In the nucleus, the labelling became restricted to the structures stained by anti-DBP antibodies, whereas labelling of the adjacent nucleoplasmic regions was totally abolished (Figure 1b, e and h). This indicates that the domains labelled by anti-DBP antibodies contain predominantly ssDNA, while the viral RNA is diffusely localized in the adjacent areas of the nucleoplasm. This is in agreement with the results obtained following digestion with DNase I: under these conditions the labelling was detected both in the cytoplasm and in the nucleus, and in the nucleus the hybridization signal was mostly excluded from the sites of ssDNA accumulation (Figure 1c and f). In conclusion, we observe that Ad2 RNA and ssDNA occupy distinct areas within the nucleus of infected cells: the ssDNA is concentrated in discrete domains labelled by anti-DBP antibodies, whereas the viral RNA is predominantly localized around these domains.

To characterize further the intranuclear pleomorphic sites of viral ssDNA accumulation, we performed serial optical sectioning using a confocal laser scanning microscope. This analysis shows that the larger structures may appear on single confocal sections as either rings or crescents (Figure 2a–c), which correspond in three dimensions to open hollow spheres or 'goblets' (not shown).

Finally, in order to visualize the total viral DNA (both double- and single-stranded), the cells were digested with RNase A and heat-denatured immediately before

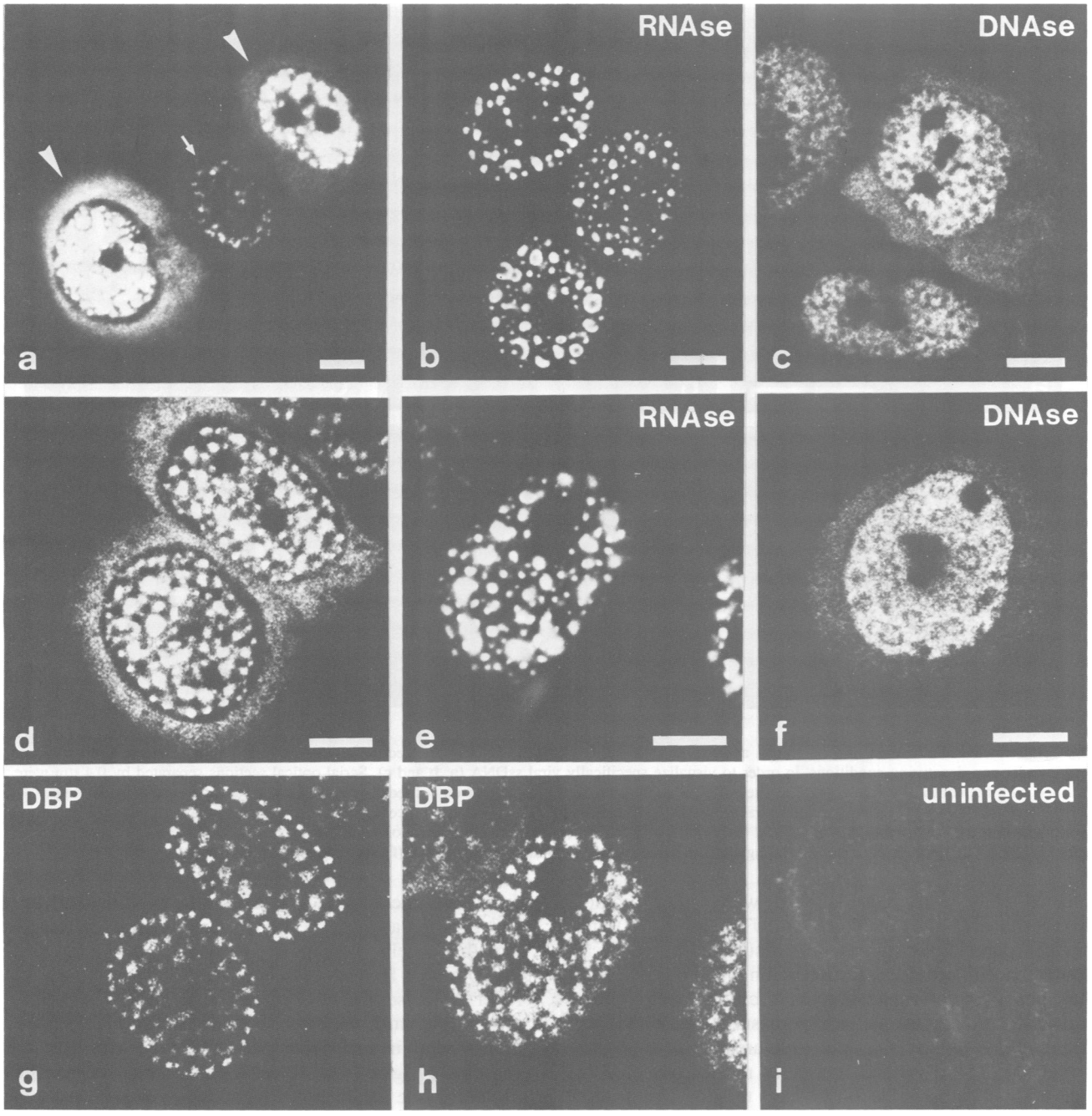

Fig. 1. *In situ* visualization of Ad2 RNA and single-stranded DNA. HeLa cells were infected for 18–20 h and hybridized *in situ* under non-denaturing conditions using a biotinylated Ad2 genomic probe. The hybridization signal is variable from cell to cell, ranging from intranuclear discrete foci (**a**, arrow) to an overall staining of both the nucleus and the cytoplasm (a, arrowheads). To characterize further the intranuclear staining, cells were hybridized with the Ad2 probe (**d**) and double-labelled with antibodies directed to the viral protein DBP (**g**). In order to visualize specifically the distribution of viral ssDNA the cells were digested with RNase A prior to hybridization (**b** and **e**) and double-labelled with anti-DBP antibodies (**e** and **h**). In order to detect viral RNA the cells were digested with DNase I prior to hybridization (**c** and **f**). As control the Ad2 probe was hybridized to mock-infected cells (**i**). Bar corresponds to 10 μm.

hybridization. At early times after infection (7–14 h), the hybridization signal was mostly restricted to tiny foci and dots in the nucleus (Figure 2d and e), as previously observed for ssDNA (Figure 1a, arrow). This indicates that at early times after infection both single- and double-stranded DNA molecules are concentrated at discrete sites in the nucleoplasm. Later, at 18–20 h post-infection, ~50% of the cells showed an overall intense labelling of the nucleoplasm (Figure 2f) and at 24 h post-infection ~90% of the cells revealed a diffuse nucleoplasmic labelling (data not shown). As ssDNA persists accumulated in discrete domains at late stages of infection (Figure 1b and e), we may conclude that dsDNA spreads progressively throughout the nucleoplasm during the course of infection.

Visualization of viral DNA replication sites

In order to correlate the intranuclear distribution of Ad2 ssDNA and dsDNA with the sites of viral replication,

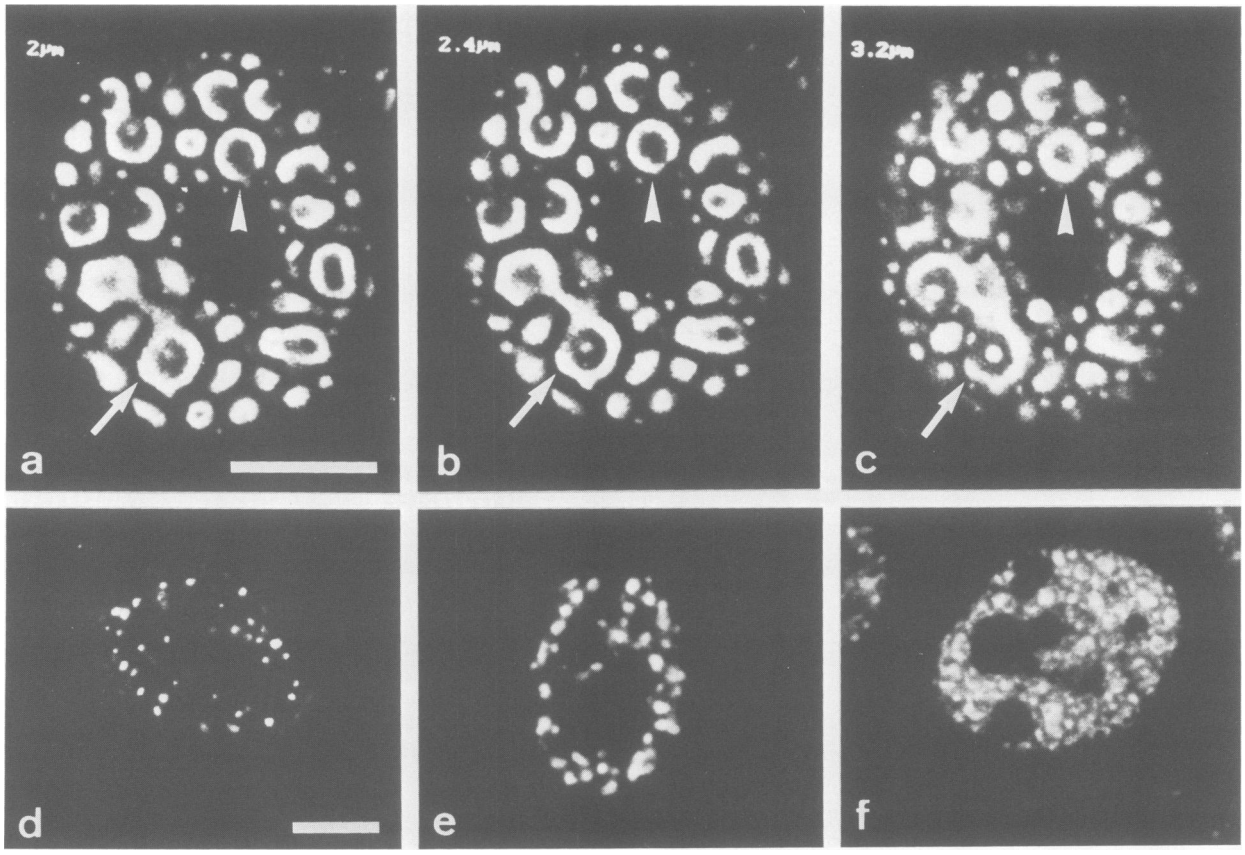

Fig. 2. Intranuclear distribution of viral single- and double-stranded DNA. HeLa cells were infected for 18 h, digested with RNase A and hybridized *in situ* under non-denaturing conditions, in order to visualize specifically viral ssDNA (**a**, **b** and **c**). Serial optical sections separated by 0.4 μm were obtained with the confocal microscope. The sites of viral ssDNA accumulation appear on consecutive optical planes as either crescents or rings (arrows and arrowheads). To visualize total viral DNA (both double- and single-stranded), the cells were digested with RNase A, heat-denatured and hybridized with the Ad2 probe (**d**, **e** and **f**). At early times of infection (7–14 h) the hybridization signal is detected as discrete foci or dots (d and e). Later (18–24 h), the labelling is detected throughout the nucleoplasm, excluding the nucleolus (f). Bar corresponds to 10 μm.

infected cells were pulse-labelled with either bromodeoxyuridine (BrdU) or biotin-16-dUTP (BiodUTP) and the incorporated nucleotides were visualized by confocal fluorescence microscopy. Both labelling methods revealed the sites of viral replication as foci that were either scattered throughout the nucleoplasm (Figure 3a) or arranged into orderly ring-like structures (Figures 3b, 3c; 4 and 5a). The dispersed foci were mostly observed in cells at 7–14 h post-infection whereas the ring-like pattern was predominantly detected at 14–24 h post-infection. Double-labelling experiments using BiodUTP and antibodies to DBP revealed that the sites of replication are associated with the structures stained by anti-DBP antibodies (Figure 3a and d, b and e, c and f), as previously reported by Bosher *et al.* (1992). However, superimposition of confocal images shows that the two labelling patterns are not completely coincident: the replication foci are predominantly localized at the surface of the structures labelled by anti-DBP antibodies (Figure 4). This was more evident at 14–24 h after infection, when the ssDNA accumulation sites became larger and clearly goblet-shaped. Note that, as the ssDNA accumulation sites form goblets (Figure 2a–c), the replication foci are detected on both the outer and inner surface of these domains (Figures 3b, 3c and 4).

As Ad replication appears to be restricted to focal sites in the nucleoplasm but the viral dsDNA is detected throughout the nucleus, it is likely that newly synthesized DNA moves away from the replication sites. To test this hypothesis cells were pulse-labelled *in vivo* with BrdU for 20 min at 16 h post-infection, and then chased for 3 h. After the pulse, the incorporated nucleotide was detected in multiple small foci arranged in rings at the periphery of the viral inclusions (Figure 5a). Following the 3 h chase, the signal was detected throughout the nucleus, excluding the nucleolus (Figure 5b). As expected, this labelling pattern is similar to that obtained by *in situ* hybridization for total viral DNA (Figure 2f). In order to exclude the possibility that the pattern of replication sites changed during the 3 h chase, cells were pulse-labelled at 19 h post-infection. This experiment revealed a distribution of replication sites similar to that observed at 16 h (data not shown). Thus, these results suggest that the pulse-labelled DNA was displaced from the replication foci and spread throughout the nucleoplasm during the 3 h chase.

Since Ad DNA replication produces single-stranded intermediates that accumulate in specific domains adjacent to the replication foci, it is likely that ssDNA molecules are also displaced from the replication foci towards these domains. We decided to confirm this hypothesis by pulse–chase experiments. Cells were pulse-labelled for 20 min at 16 h post-infection and chased for 3 h. The incorporated BrdU was then detected in the absence of acid-denaturation (Figure 5c). Since treatment with acid is

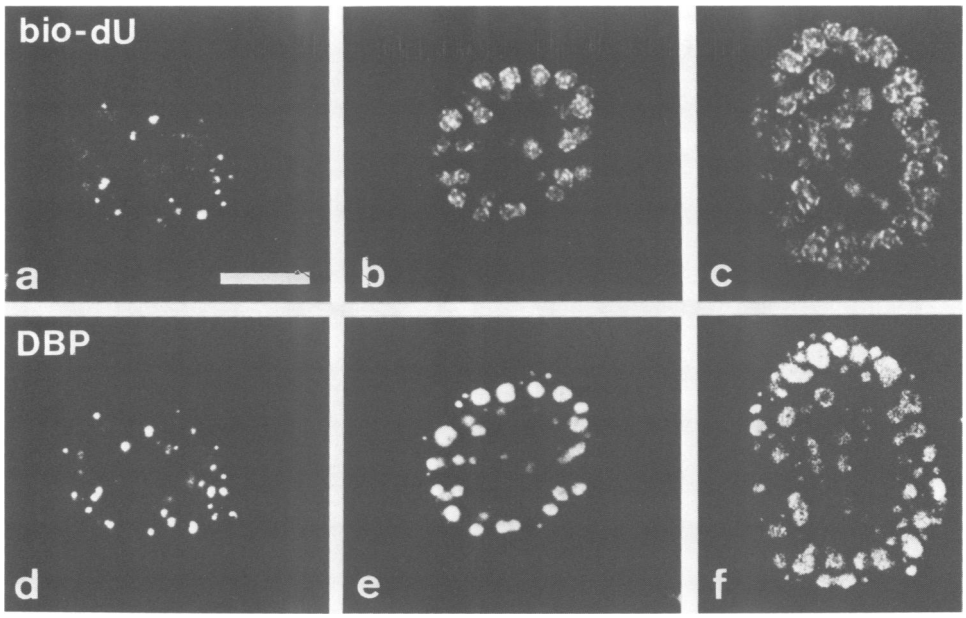

Fig. 3. Visualization of Ad replication sites. HeLa cells were infected for 18–20 h, incubated with biotin-dUTP for 10 min (**a**, **b** and **c**) and double-labelled with anti-DBP antibodies (**d**, **e** and **f**). At this time of infection the majority of cells contain multiple replication foci arranged in rings around the structures stained by anti-DBP antibodies (b and e, c and f). In a small percentage of cells the sites of replication are visualized as discrete dots scattered throughout the nucleoplasm (a), which are also labelled by anti-DBP antibodies (d). Bar corresponds to 10 μm.

required for antibodies to have access to BrdU incorporated into double-stranded DNA (Nakamura *et al.*, 1986), in the absence of acid-denaturation the anti-BrdU antibodies should bind preferentially to single-stranded molecules. As expected, when the acid treatment was omitted the incorporated BrdU was exclusively detected within the structures labelled by anti-DBP antibodies (Figure 5c and d).

In summary, the data provide evidence that the single- and double-stranded viral DNA molecules are differentially displaced from the sites of replication: the single-stranded intermediates become accumulated in discrete adjacent domains, whereas the double-stranded molecules spread throughout the nucleoplasm.

Visualization of viral RNA transcription sites

The sites of transcription within the nucleus of infected HeLa cells were visualized by fluorescence microscopy following incorporation of bromo-UTP (Figure 6). At 8 h post-infection the distribution of transcription sites in the nucleus of most infected cells was similar to that observed in uninfected cells, i.e. a multitude of small foci widely spread throughout the nucleoplasm (Figure 6a and d), corresponding to the sites of host cellular transcription as previously described (Jackson *et al.*, 1993; Wansink *et al.*, 1993). At later times of infection (10–14 h), a progressively higher percentage of cells had a non-homogeneous distribution of transcription sites, which appeared more intensely labelled and concentrated around the inclusions labelled by anti-DBP antibodies (Figure 6b and e). Later (16–20 h), the transcription sites in most cells were very intensely labelled and distributed around the large viral inclusions labelled by anti-DBP antibodies (Figure 6c and f). This distribution is strikingly similar to that obtained after *in situ* hybridization to viral RNA (compare Figure 6c with Figure 1f).

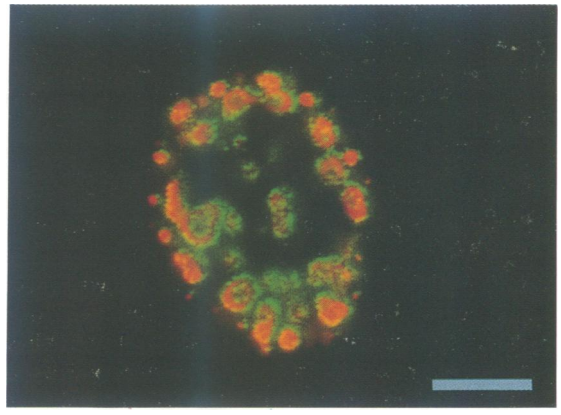

Fig. 4. Intranuclear organization of replication foci. HeLa cells were infected for 20 h, incubated with biotin-dUTP for 15 min (green staining) and double-labelled with anti-DBP antibodies (red staining). Pseudo-colour images obtained in the same optical plane were recorded and superimposed. Note that the replication foci are detected at the periphery of the goblet-shaped structures labelled by anti-DBP antibodies. Bar corresponds to 10 μm.

As control experiments, the transcription assay was performed in the presence of 100 μg/ml α-amanitin, which selectively inhibits RNA polymerases II and III (Sarin and Gallo, 1980). Under these conditions transcription was detected exclusively in the nucleolus (Figure 6g and i). Alternatively, the transcription assay was performed in the presence of 1 μg/ml α-amanitin, in order to inhibit RNA polymerase II only. Under these conditions transcription sites were observed in the nucleolus and in a restricted number of nucleoplasmic foci (Figure 5h), which probably correspond to sites of viral transcription by RNA polymerase III. When the transcription assay was performed in the presence of both 100 μg/ml α-amanitin (to inhibit RNA polymerases II and III) and 0.08 μg/ml actinomycin

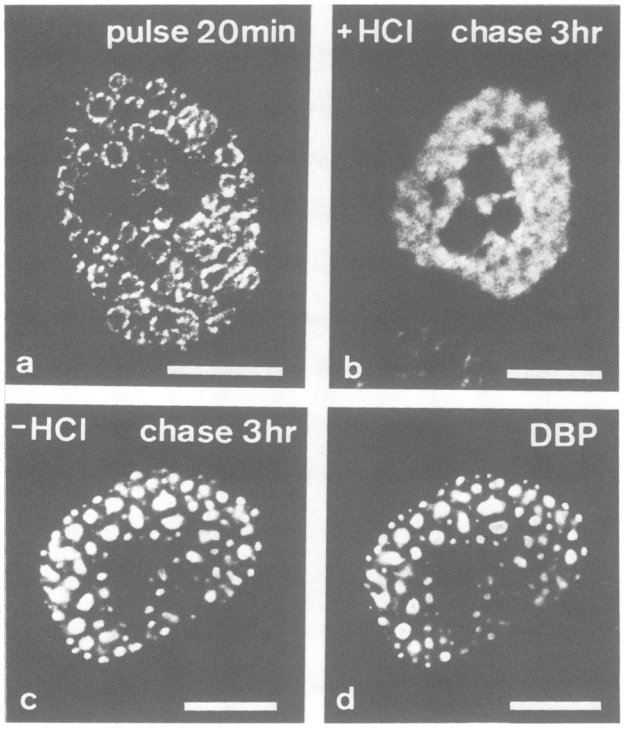

Fig. 5. Visualization of Ad DNA movement in the nucleus. Cells were infected for 16 h and pulse-labelled *in vivo* with bromo-dU for 20 min. After the pulse, the cells were either immediately fixed and analyzed (**a**) or chased for 3 h (**b** and **c**). Following the chase, the incorporated bromo-dU was detected in either the presence (b) or absence (c) of acid-treatment. When the acid treatment was omitted the cells were double-labelled with anti-DBP antibodies (**d**). Bar corresponds to 10 μm.

D (to inhibit RNA polymerase I) the labelling was totally abolished (Figure 6j).

In summary, the data indicate that the widespread nucleoplasmic labelling concentrated in rims around the viral inclusions represents primarily transcription by RNA polymerase II. Since viral mRNA is transcribed by the host cellular RNA polymerase II and the cellular messages continue to be synthesized at nearly normal levels (Beltz and Flint 1979), it is not possible to identify specifically the sites of viral versus host transcription. However, the increase in signal intensity and concentration around the viral domains labelled by anti-DBP antibodies, strongly suggests that these sites correspond to viral mRNA transcription.

Simultaneous visualization of viral replication and transcription

Having established the intranuclear distribution of Ad transcription and replication, we next addressed the question of whether the sites of viral DNA and RNA synthesis co-localize *in vivo*. HeLa cells were simultaneously incubated with BiodUTP and BrUTP and the intranuclear sites of replication and transcription were then visualized by, respectively, rhodamine-labelled extravidin and fluorescein-labelled antibodies (Figure 7).

The sites of viral transcription (Figure 7a, d, g, c, f and i, green staining) and replication (Figure 7b, e, h, c, f and i, red staining) appeared closely associated but not coincident. Thus, RNA transcription occurs in close proximity to the sites of DNA replication. However, the sites of transcription are detected adjacent to the replication foci and occupy a more extensive area, which increases progressively throughout the course of infection (Figure 7c, f and i). This suggests that, as new DNA is synthesized in the replication foci, the older molecules are pushed into the surrounding nucleoplasm where they serve as templates for transcription.

Splicing snRNPs co-localize with sites of viral RNA transcription and are not detected in replication foci

Since the adenovirus makes use of the host cellular splicing machinery for processing of its mRNAs, we were interested in comparing the spatial distribution of snRNPs with the sites of viral transcription and of viral replication. Cells at 18–20 h post-infection were incubated with either BrUTP or BiodUTP and then immunolabelled with anti-Sm antibodies. The results show co-localization of snRNPs with the sites of transcription in the nucleoplasm (Figure 8a). In contrast, snRNPs were predominantly excluded from the replication foci (Figure 8b). This indicates that snRNPs become concentrated at the sites of nascent viral transcripts, suggesting that splicing of Ad mRNAs is co-transcriptional in agreement with data obtained in non-infected cells (Beyer and Osheim, 1988; LeMaire and Thummel, 1990). Furthermore, these results provide further evidence that adenovirus DNA replication is spatially separated from RNA transcription and processing in the nucleus of infected cells.

Discussion

In this work we provide evidence that replication of Ad DNA is spatially separated from Ad RNA transcription in the nucleus of infected HeLa cells. Replication of Ad DNA is shown to occur in multiple foci whereas transcription is detected in adjacent areas of the nucleoplasm. As the newly synthesized viral dsDNA molecules are shown to be displaced from the replication foci and spread into the adjacent nucleoplasm, the data indicate that the displaced dsDNA molecules are used as templates for transcription.

Previous light and electron microscopic studies have established that the nuclei of adenovirus-infected cells contain several morphologically distinct inclusions (Martinez-Palomo *et al.*, 1967; Sugawara *et al.*, 1977; Moyne *et al.*, 1978; Reich *et al.*, 1983; Puvion-Dutilleul *et al.*, 1984; Voelkerding and Klessig, 1986; Murti *et al.*, 1990). Among these inclusions, particular attention has been focused on pleomorphic structures that contain DBP, a viral protein required for DNA replication (see Challberg and Kelly, 1989). At the ultrastructural level, DBP has been predominantly detected in compact fibrillar structures with the shape of rings, crescents or spheres (Puvion-Dutilleul *et al.*, 1984). Since these structures also accumulate viral ssDNA, they have been named ssDNA accumulation sites (Puvion-Dutilleul and Puvion, 1990a,b). Here we performed serial optical sectioning and 3-dimensional reconstruction and show that the ssDNA accumulation sites are goblet-shaped.

At the light microscopic level, Bosher *et al.* (1992) have previously reported that the structures labelled by anti-DBP antibodies correspond to DNA replication cen-

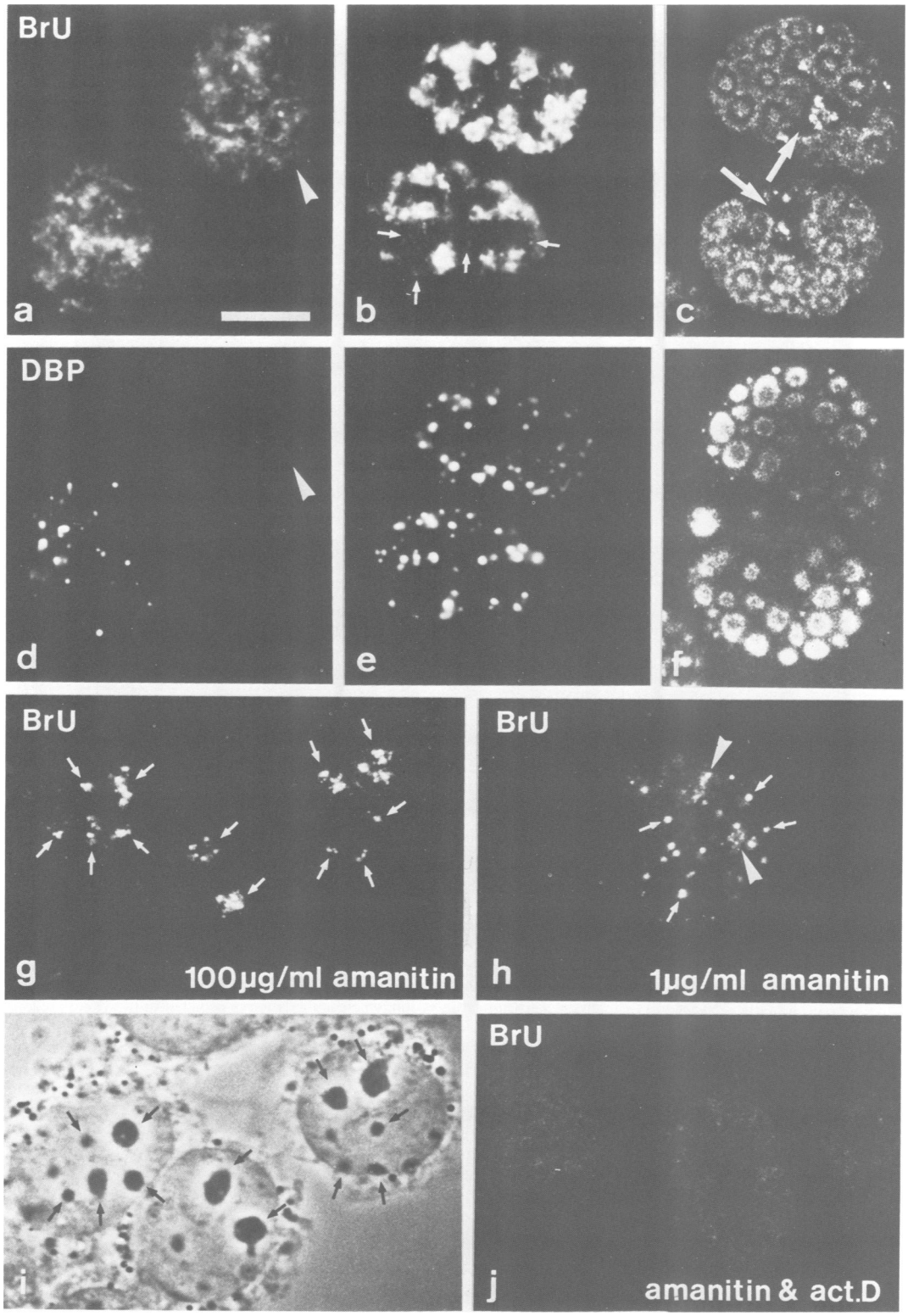

Fig. 6. Visualization of Ad transcription sites. HeLa cells infected for 8–20 h were incubated with bromo-UTP for 10 min (**a**, **b** and **c**) and double-labelled with anti-DBP antibodies (**d**, **e** and **f**). Between 8 and 14 h post-infection, the cells are either labelled with a pattern similar to non-infected cells, i.e. a multitude of foci widely spread throughout the nucleoplasm (a), or show several discrete and intensely labelled areas (b). In (a and d) the arrowhead points to a cell that is not labelled by anti-DBP antibodies, either because it has not been infected or it is in a very early stage of infection. In (b) the mostly intensely labelled areas have a distribution similar to that of viral structures labelled by anti-DBP antibodies (e); in addition to these intensely labelled areas, there are small foci scattered in the nucleoplasm that may correspond to sites of host cellular transcription (b, arrowheads). At 16–20 h post-infection, in most cells the incorporated UTP is predominantly detected at the periphery of the goblets stained by anti-DBP antibodies (c and f); in addition, labelling is also observed in the nucleolus (c, arrows). As controls, cells were incubated with bromo-UTP in the presence of specific inhibitors of transcription. In the presence of 100 µg/ml α-amanitin, the labelling is restricted to the nucleolus, as confirmed by phase contrast microscopy (**g** and **i**, arrows). In the presence of 1 µg/ml α-amanitin the labelling is detected in the nucleolus (**h**, arrowheads) and in several nucleoplasmic foci (h, arrows). In the presence of both α-amanitin (100 µg/ml) and actinomycin D (0.08 µg/ml) no signal is observed (**j**). Bar corresponds to 10 µm.

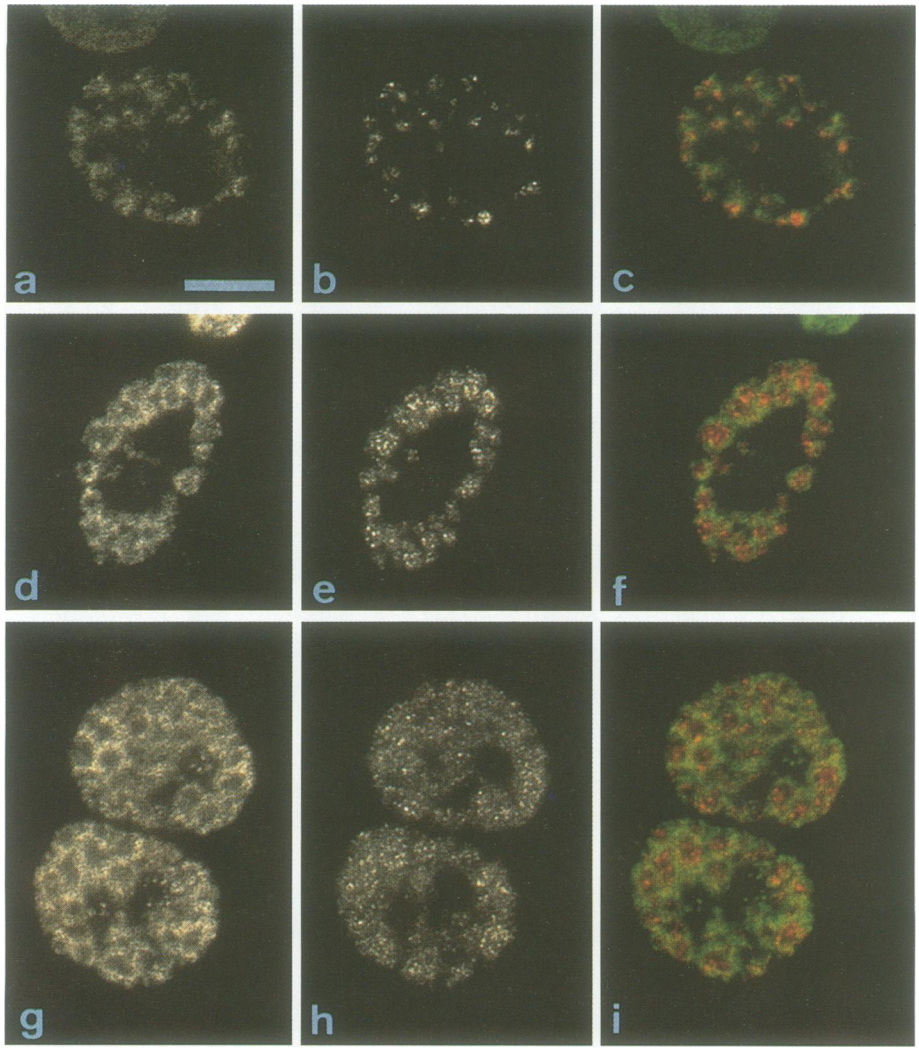

Fig. 7. Simultaneous visualization of viral transcription and replication. Infected HeLa cells were simultaneously incubated with bromo-UTP and biotin-dUTP for 15 min. The sites of transcription were visualized using fluorescein-conjugated antibodies (**a**, **d** and **g**) and replication sites were detected with rhodamine-extravidin (**b**, **e** and **h**). Pseudo-colour images were generated and superimposed (**c**, **f** and **i**). The colour images show that the sites of transcription and replication occupy distinct, but closely associated areas in the nucleus (note separate red and green staining). The labelling pattern depicted in (a–c) is representative of cells at 7–14 h post-infection, whereas the patterns depicted in (d–i) are predominantly observed at 16–20 h post-infection. Bar corresponds to 10 μm.

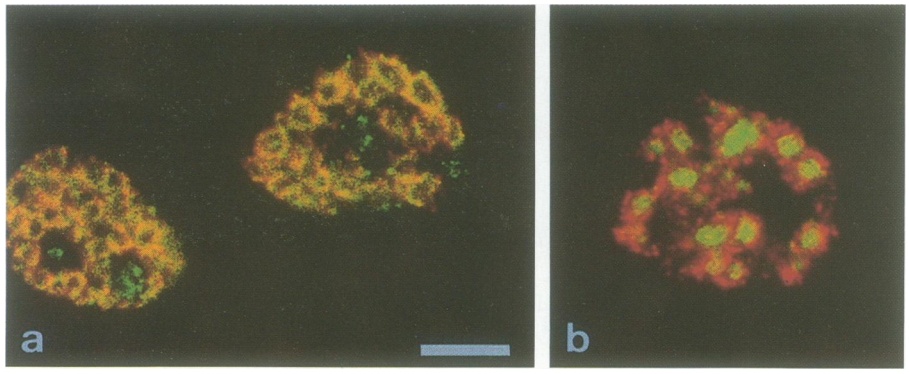

Fig. 8. Splicing snRNPs concentrate at the sites of viral transcription and are excluded from replication foci. HeLa cells infected for 18 h were incubated with either bromo-UTP (**a**) or biotin-dUTP (**b**) and double-labelled with anti-Sm human autoantibodies. The incorporated nucleotides were visualized using a fluorescein-conjugated secondary antibody (a and b, green staining), and snRNPs were visualized using a Texas red-conjugated secondary antibody (a and b, red staining). Confocal images from each fluorochrome were recorded and superimposed. The labelling produced by anti-Sm antibodies co-localizes with transcription sites in the nucleoplasm (a, the yellow colour is due to overlapping of red and green staining), but not in the nucleolus (a, arrows: green staining). In contrast, the labelling produced by anti-Sm antibodies does not co-localize with replication sites (b, red and green staining). Bar corresponds to 10 μm.

ters. Making use of the higher resolution capacity of the confocal microscope, we show that the sites of Ad replication and the structures labelled by anti-DBP antibodies are associated, but do not co-localize precisely (Figure 4). At the electron microscopic level, Puvion-Dutilleul and Puvion (1990b; 1991) have distinguished early and late replicative sites by using [^{3}H]thymidine incorporation and autoradiography. The early replicative sites were described as fibrillar masses containing ds and ssDNA, and the late replicative sites or 'peripheral replicative zones' consisted of fibrillogranular material surrounding the ssDNA accumulation sites. Likely, the replication foci that we observe dispersed throughout the nucleus of cells infected for 7–14 h correspond to the early replicative sites, whereas the replication foci arranged in ring-like structures at the periphery of the ssDNA accumulation sites (i.e. the structures labelled by anti-DBP antibodies) correspond to the peripheral replicative zones.

It has been suggested previously that in eukaryotic cells active DNA polymerases are clustered into 'replication factories' attached to a nucleoskeleton (Laskey *et al.*, 1989; Berezney, 1991; Cook, 1991) and that replication may occur as the template moves through the factories (Hozák *et al.*, 1993). According to this view, each focus that incorporates thymidine analogues in the nucleus of infected cells may represent one viral replication factory and their highly ordered arrangement at the periphery of discrete domains may reflect an association with an underlying scaffold.

In contrast with the eukaryotic chromosomes which occupy specific 'territories' in the nucleus (Cremer *et al.*, 1994), Ad DNA is detected throughout the nucleoplasm. As the replication foci appear to occupy fixed positions at the periphery of discrete nucleoplasmic domains, then the viral DNA molecules are likely to move in the nucleus. The results from pulse–chase experiments confirm that newly synthesized dsDNA spreads from the replication foci to the surrounding nucleoplasm, whereas the ssDNA is displaced into adjacent accumulation sites. One simple explanation for this movement is that the newly synthesized DNA molecules displace the pre-existing ones. This is consistent with the observation that replication foci can only be clearly resolved from sites of ssDNA and dsDNA accumulation at later times of infection. Independently of the driving force, the viral genomes probably do not diffuse freely in the nucleus, since Ad DNA is tightly bound to the nuclear matrix throughout the course of infection (Schaack *et al.*, 1990; Fredman and Engler, 1993). The sites of tightest attachment occur in the terminal fragments of the linear viral chromosome and are mediated by the viral terminal protein, which is covalently bound to the 5′ end of each DNA strand (Schaack *et al.*, 1990, Fredman and Engler, 1993).

Although biochemical studies indicate that Ad replicating DNA molecules are not templates for transcription (Brison *et al.*, 1979), several authors performing electron microscope analysis of spread adenovirus DNA molecules have shown that replication and transcription can occur in the same molecule (Matsuguchi and Puvion-Dutilleul, 1980; Beyer *et al.*, 1981; Wolgemuth and Hsu, 1981). The simultaneous visualization of replication and transcription in the nucleus of infected cells shows that the two processes are closely associated *in vivo* but do not perfectly co-localize (note separate red and green staining in Figure 7). Transcription is predominantly detected separate from the sites of replication, although the resolution and sensitivity limits of the fluorescence microscope do not allow to exclude that some viral RNA synthesis occurs on replicating DNA molecules. The sites of transcription occupy progressively larger areas at later times of infection, consistent with the observation that dsDNA templates spread from the replication foci into the surrounding nucleoplasm.

The finding that the sites of Ad transcription do not co-localize with the sites of replication contrasts with the recent report that replication initiates only at transcription sites in non-infected HeLa cells (Hassan *et al.*, 1994), although a more recent study indicates that in S-phase nuclei of human bladder carcinoma cells transcription and replication domains do not co-localize (Wansink *et al.*, 1994). However, it is important to note that the mechanisms responsible for Ad DNA synthesis are quite distinct from those involved in mammalian chromatin replication. Namely, Ad DNA replication is initiated by a protein priming mechanism and the daughter strands are elongated by a continuous mode of synthesis which produces displaced single-stranded intermediates (reviewed by Challberg and Kelly, 1989). Therefore it is not surprising that the intranuclear organization of Ad replication and transcription sites may differ from that of mammalian cells.

Previous studies have demonstrated that Ad causes a drastic redistribution of several host cellular factors including the transcription factor NFI, nucleolar proteins and snRNPs (Walton *et al.*, 1989; Bosher *et al.*, 1992; Bridge *et al.*, 1993; Jiménez-Garcia and Spector, 1993). In particular, the splicing factor SC-35 and snRNPs have been reported to be relocalized to the sites of viral RNA and ssDNA accumulation (Jiménez-Garcia and Spector, 1993). However, these results should be cautiously interpreted as more recent studies indicate that the anti-SC-35 monoclonal antibody cross-reacts with the viral protein DBP (Bridge *et al.*, submitted). In the present work we show that the sites of RNA transcription are clearly distinct from the structures labelled by anti-DBP antibodies, which correspond to sites of ssDNA accumulation. In addition, the results demonstrate that splicing snRNPs become concentrated at the sites of viral transcription. This indicates that snRNPs associate with nascent viral transcripts and suggests that splicing of Ad pre-mRNAs may occur co-transcriptionally. This view is consistent with previous data from eukaryotic cells indicating that splicing occurs on nascent transcripts (for review see Rosbach and Singer, 1993). However, the re-localization of snRNPs to the sites of viral transcription is a transient process observed in cells at intermediate stages of infection (12–18 h post-infection). At later times (18–24 h post-infection), snRNPs become accumulated in large clusters of interchromatin granules (Bridge *et al.*, 1993), suggesting that some change in viral RNA metabolism occurs at this stage (Bridge *et al.*, submitted).

The observation that splicing snRNPs redistribute in the nucleus of infected cells to the sites of transcription and are not detected in the sites of replication provides further evidence that viral replication is spatially separated from RNA transcription and processing. This could imply the existence of separate 'factories' for DNA replication

and RNA transcription/processing which would occupy distinct fixed positions in the nucleus, and therefore the viral DNA templates have to move from the sites of replication to the sites of transcription and processing. However, there is evidence that both replication and transcription can occur in the same viral template (Matsuguchi and Puvion-Dutilleul, 1980; Beyer *et al.*, 1981; Wolgemuth and Hsu, 1981), arguing that both machineries may co-localize in the nucleus. Possibly, the transcription and processing of Ad RNA is primarily dependent upon the presence of templates in the nucleus and therefore it can occur either when the dsDNA is still associated with the replication site or when it is spread out in the nucleoplasm.

A major conclusion from this work is that replication, transcription and processing of simple viral genomes introduced into a mammalian cell are not randomly localized in the nucleus. Rather, these processes require a precise spatial organization which involves a defined trafficking of specific molecules in the nucleoplasm. Hopefully, future studies using mutant virus defective for either DNA replication or RNA transcription and processing may help to elucidate the intricate relations between nuclear structure and function in mammalian cells.

Materials and methods

Cell culture and adenovirus infection

HeLa cell monolayer cultures were maintained in Dulbecco's modified minimum essential medium supplemented with 10% fetal calf serum. Subconfluent cells were infected with wild-type Ad2 at a multiplicity of infection of 20 focus forming units (f.f.u.) per cell. Virus titers, expressed as f.f.u./ml, were determined on HeLa monolayers as described (Philipson, 1961). The cells were inoculated with virus in serum-free medium. After incubation for 1–2 h, the medium was removed and replaced by fresh medium supplemented with 10% serum until the time for fixation. The virus added was sufficient to infect >90% of cells in all experiments.

Immunofluorescence

Ad2 and mock infected HeLa cells were grown on glass coverslips and harvested at various times post-infection. The cells were washed twice in phosphate buffered saline (PBS) and subsequently fixed in 3.7% paraformaldehyde in CSK buffer (Fey *et al.*, 1986) for 10 min at room temperature. After fixation, the cells were permeabilized with 0.5% Triton X-100 in CSK buffer for 15 min at room temperature. Alternatively, the cells were washed twice with PBS, permeabilized with 0.5% Triton X-100 in CSK buffer containing 0.1 mM PMSF for 1 min on ice, and then fixed in 3.7% paraformaldehyde in CSK buffer for 10 min at room temperature. After fixation and permeabilization the cells were rinsed in PBS containing 0.05% Tween 20, incubated for 1 h with primary antibodies diluted in PBS containing 0.05% Tween 20, washed in PBS containing 0.05% Tween 20 and incubated with secondary antibodies for 1 h. Secondary antibodies conjugated to FITC or Texas red were obtained from Dianova (Germany). Finally, the samples were mounted in VectaShield (Vector Laboratories, UK).

The following antibodies were used: rabbit antibodies raised against the viral protein DBP, human autoantibodies specific for Sm snRNP proteins and the anti-Sm monoclonal antibody Y12 (Lerner *et al.*, 1981; Pettersson *et al.*, 1984).

In situ hybridization

Ad2 genomic DNA (1 μg) was labelled by nick translation in the presence of 0.06 mM biotin-16-dUTP (Boehringer Mannheim Biochemicals, Germany) as described by Johnson *et al.* (1991). The resulting fragments were monitored by agarose gel electrophoresis and the reaction was stopped when fragments of ~200 bp were obtained. The probe was then purified through a G-50 Sephadex column (Boehringer).

For *in situ* hybridization the cells were fixed in 3.7% paraformaldehyde in CSK buffer for 10 min and then permeabilized by incubation with 0.05% SDS in 100 mM Tris–HCl, pH 7.5, 150 mM NaCl, 12.5 mM EDTA for 5 min with gentle shaking. For hybridization under non-denaturing conditions, the cells were washed twice with 2× SSC, rinsed with 2× SSC containing 0.05% Tween 20 and incubated with hybridization mixture (8 μl per coverslip) for 1 h at 37°C, in a moist chamber. For detection of viral double-stranded DNA, the cells were washed twice in 2× SSC, incubated with 50% formamide in 2× SSC at 90°C for 10 min, washed in ice-cold 2× SSC, and incubated with the hybridization mixture.

The hybridization mixture was prepared by dissolving (per coverslip) 36 ng of biotinylated Ad2 total genomic probe and 8 μg of competitor *E.coli* tRNA in 4 μl of deionized formamide. The probe was denatured by heating for 10 min at 70°C and immediately chilled on ice. Then, dextran sulfate and SSC were added. The final concentrations in the hybridization mixture were: 4 ng/μl Ad2 biotinylated DNA, 1 μg/μl *E.coli* tRNA, 2× SSC, 10% dextran sulfate and 50% deionized formamide.

After hybridization, the cells were successively washed in 50% formamide in 2× SSC for 15 min at 37°C, 2× SSC for 30 min at room temperature and finally 1× SSC for 15 min at room temperature. Then the cells were rinsed in 20 mM HEPES, pH 7.9, 150 mM KCl, 0.05% Tween 20 (avidin wash buffer) and incubated with FITC-conjugated extravidin (Sigma) for 1 h at room temperature. The extravidin was used at a concentration of 2 μg/ml in 20 mM HEPES, pH 7.9, 250 mM KCl, 0.5 mM DTT, 1% BSA. After washing in avidin wash buffer, the samples were either immunolabelled and mounted or directly mounted in VectaShield.

Human placental ribonuclease inhibitor (RNAsin, Amersham, UK) was added to all washing solutions to a final concentration of 2.5 U/ml, except when the samples were previously digested with RNase A.

Nuclease digestion was performed on cells fixed in paraformaldehyde and permeabilized with SDS, before hybridization. For DNase treatment, the cells were washed twice with DNase buffer (10 mM Tris–HCl, pH 7.5, 25 mM $MgCl_2$, 2 mM DTT) and incubated with 200 U/ml DNase I (FPLC pure™, Pharmacia LKB Biotechnology, Sweden) in DNase buffer containing 50 U/ml RNAsin, at 37°C for 2 h. For RNase treatment, the cells were washed twice with 10 mM Tris–HCl, pH 7.5 and incubated with 200 μg/ml RNase A (Sigma) in the same buffer, at 37°C for 1 h.

Visualization of replication sites

Cells were pulse-labelled *in vivo* with 150 mM bromodeoxyuridine (BrdU, Boehringer) for 20 min, or alternatively, pulse-labelled for 20 min and chased for 3 h. For detection of BrdU incorporated into dsDNA, the cells were washed with PBS, fixed in pre-cooled 70% ethanol, 50 mM glycine, pH 2.0 for 20 min at −20°C, rinsed in PBS, incubated with 4 N HCl for 30 min and finally washed in PBS (Nakamura *et al.*, 1986). For detection of BrdU incorporated exclusively in ssDNA the acid treatment was omitted. The cells were then blocked with 5% fetal calf serum in PBS for 15–30 min, washed in PBS, incubated with anti-bromodeoxyuridine primary antibody (Boehringer), blocked again with 5% fetal calf serum in PBS for 15–30 min, washed and finally incubated with a secondary antibody coupled to FITC (Dianova). In some experiments the infected cells were incubated with 5 μg/ml aphidicolin for 14 h prior to the *in vivo* pulse with BrdU. Aphidicolin is a specific inhibitor of DNA polymerase α but at this concentration does not inhibit the Ad2 DNA polymerase (Kwant and van der Vliet, 1980). Control experiments demonstrated that treatment with aphidicolin under these conditions abolishes incorporation of BrdU into uninfected cells but does not affect detection of viral replication. However, treatment with 10 mM hydroxyurea for 3 h prior to the pulse totally blocked incorporation of BrdU into infected cells.

Alternatively, cells on coverslips were permeabilized with 0.05% Triton X-100 in the physiological buffer (PB) described by Jackson *et al.* (1993) for 1–2 min at 4°C and incubated with 0.1 mM biotin-16-dUTP (Boehringer) for 10–20 min at 33°C, as described by Hozák *et al.* (1993). Biotin was detected using extravidin conjugated to either fluorescein or rhodamine (Sigma) as described for *in situ* hybridization. After the replication reaction and detection, the samples were either immediately mounted or first immunolabelled with anti-DBP or anti-Sm antibodies and then mounted.

Visualization of transcription sites

Visualization of transcription sites was performed essentially according to Jackson *et al.* (1993). Briefly, cells grown as monolayers on coverslips were permeabilized with 0.05% Triton X-100 in PB buffer for 1–2 min at 4°C and incubated with 0.1 mM bromo-UTP (Sigma) for 10–20 min

at 33°C. Incorporated bromo-UTP was detected using a primary antibody anti-bromodeoxyuridine (Boehringer Mannheim) and a secondary antibody coupled to FITC (Dianova). If added, α-amanitin (1 or 100 μg/ml) or actinomycin D (0.08 μg/ml) were present for 10 min at 4°C prior to, and during, transcription. After the transcription reaction and detection, the samples were either immediately mounted or first immunolabelled with anti-DBP or anti-Sm antibodies and then mounted.

For the simultaneous visualization of transcription and replication sites the cells were permeabilized with 0.05% Triton X-100 in PB (Jackson *et al.*, 1993) and incubated with 0.1 mM biotin-16-dUTP and 0.1 mM bromo-UTP for 10–20 min at 33°C. The incorporated nucleotides were then detected using, respectively, FITC–conjugated secondary antibody and rhodamine–extravidin.

Confocal microscopy

Cells were examined with a Zeiss Laser Scanning Microscope (LSM 310) using an Argon Ion laser (488 nm) to excite FITC fluorescence and a Helium/Neon laser (543 nm) to excite Texas red and rhodamine fluorescence. Images were photographed on Fujichrome 100 or Kodak TMax100 film, using a Polaroid freeze frame recorder.

Acknowledgements

The authors are grateful to Dr A.Lamond for critical reading of the manuscript and to Prof. U.Pettersson for support. We thank Dr T.Linné for providing anti-DBP antibodies and Dr I.Mattaj for providing the anti-Sm human serum 'Küng' and the monoclonal antibody Y12. We are also thankful to Martins Lemos Audiovisuais for help in photographic work. This work was supported by grants from Junta Nacional de Investigação Científica e Tecnológica, EC, Swedish Medical Research Council and Uppsala University.

References

Beltz,G.A. and Flint,S.J. (1979) *J. Mol. Biol.*, **131**, 353–373.
Berezney,R. (1991) *J. Cell. Biochem.*, **47**, 109–123.
Beyer,A.L. and Osheim,Y.N. (1988) *Genes Dev.*, **2**, 754–765.
Beyer,A.L., Bouton,A.H., Hodge,L.D. and Miller,O.L. (1981) *J. Mol. Biol.*, **147**, 269–295.
Bosher,J., Dawson,A. and Hay,R.T. (1992) *J. Virol.*, **66**, 3140–3150.
Bridge,E., Carmo-Fonseca,M., Lamond,A.I. and Pettersson,U. (1993) *J. Virol.*, **67**, 5792–5802.
Brison,O., Kedinger,C. and Chambon,P. (1979) *J. Virol.*, **32**, 91–97.
Challberg,M.D. and Kelly,T.J. (1989) *Annu. Rev. Biochem.*, **58**, 671–717.
Cook,P.R. (1991) *Cell*, **66**, 627–635.
Cremer,T. *et al.* (1994) *Cold Spring Harbor Symp. Quant. Biol.*, **58**, 777–792.
Darnell,J.E.,Jr (1982) *Nature*, **297**, 365–371.
Fey,E.G., Krochmalnic,G. and Penman,S. (1986) *J. Cell Biol.*, **102**, 1654–1665.
Flint,S.J. (1986) *Adv. Virus Res.*, **31**, 169–228.
Fredman,J.N. and Engler,J.A. (1993) *J. Virol.*, **67**, 3384–3395.
Greber,U.F., Willetts,M., Webster,P. and Helenius,A. (1993) *Cell*, **75**, 477–486.
Hassan,A.B., Errington,R.J., White,N.S., Jackson,D. and Cook,P. (1994) *J. Cell Sci.*, **107**, 425–434.
Horwitz,M.S. (1990) In Fields,B.N. and Knipe,D.M. (eds), *Virology*. Raven Press, New York, vol. I, pp. 1679–1721.
Hozák,P., Hassan,A.B., Jackson,D.A. and Cook,P.R. (1993) *Cell*, **73**, 361–373.
Jackson,D.A. (1991) *Bioessays*, **13**, 1–10.
Jackson,D.A., Hassan,A.B., Errington,R.J. and Cook,P.R. (1993) *EMBO J.*, **12**, 1059–1065.
Jiménez-Garcia,L.F. and Spector,D.L. (1993) *Cell*, **73**, 47–59.
Johnson,C.V., Singer,R.H. and Lawrence,J.B. (1991) *Meth. Cell Biol.*, **35**, 73–98.
Kwant,M.M. and van der Vliet,P.C. (1980) *Nucleic Acids Res.*, **8**, 3993.
Laskey,R.A., Fairman,M.P. and Blow,J.J. (1989) *Science*, **246**, 609–614.
LeMaire,M.F. and Thummel,C.S. (1990) *Mol. Cell. Biol.*, **10**, 6059–6063.
Lerner,E.A., Lerner,M.R., Janeway,C.A.,Jr and Steitz,J.A. (1981) *Proc. Natl Acad. Sci. USA*, **78**, 2737–2741.
Martin,T.E., Barghusen,S.C., Leser,G.P. and Spear,P.G. (1987) *J. Cell Biol.*, **105**, 2069–2082.
Martinez-Palomo,A., Le Buis,J. and Bernhard,W. (1967) *J. Virol.*, **1**, 817–829.
Mathews,M.B. and Shenk,T. (1991) *J. Virol.*, **65**, 5657–5662.
Matsuguchi,M. and Puvion-Dutilleul,F. (1980) *Biol. Cell.*, **39**, 187–190.
Moran,E. (1993) *FASEB J.*, **7**, 880–885.
Moyne,G., Pichard,E. and Bernhard,W. (1978) *J. Gen. Virol.*, **40**, 77–92.
Mulligan,R.C. (1993) *Science*, **260**, 926–932.
Murti,K.G., Davis,D.S. and Kitchingman,G.R. (1990) *J. Gen. Virol.*, **71**, 2847–2857.
Nakamura,H., Morita, T and Sato,C. (1986) *Exp. Cell Res.*, **165**, 291–297.
Pettersson,I., Hinterberger,M., Mimori,T., Gottlieb,E. and Steitz,J.A. (1984) *J. Biol. Chem.*, **259**, 5907–5914.
Phelan,A., Carmo-Fonseca,M., McLauchlan,J., Lamond,A., I. and Clements,J.B. (1993) *Proc. Natl Acad. Sci. USA*, **90**, 9056–9060.
Philipson,L. (1961) *Virology*, **15**, 263–268.
Philipson,L., Pettersson,U. and Lindberg,U. (1975) *Virology Monographs.* **14**, Springer-Verlag, Wien, pp. 1–115.
Puvion-Dutilleul,F. and Puvion,E. (1990a) *Eur. J. Cell Biol.*, **52**, 379–388.
Puvion-Dutilleul,F. and Puvion,E. (1990b) *J. Struct. Biol.*, **103**, 280–289.
Puvion-Dutilleul,F. and Puvion,E. (1991) *Biol. Cell*, **71**, 135–147.
Puvion-Dutilleul,F., Pédron,J. and Cajean-Feroldi,C. (1984) *Eur. J. Cell Biol.*, **43**, 313–322.
Puvion-Dutilleul,F. and Christensen,M.E. (1993) *Eur. J. Cell Biol.*, **61**, 168–176.
Reich,N.C., Sarnow,P., Duprey,E. and Levine,A.J. (1983) *Virology*, **128**, 480–484.
Rosbach,M. and Singer,R.H. (1993) *Cell*, **75**, 399–401.
Sarin,P.S. and Gallo,R.C. (1980) *Inhibitors of DNA and RNA polymerases.* Pergamon Press, Oxford.
Schaack,J., Ho,W.Y.-W., Freimuth,P. and Shenk,T. (1990) *Genes Dev.*, **4**, 1197–1208.
Sharp,P.A. (1984) In Ginsberg,H.S. (ed.) *The adenovirus.* Plenum Press, New York, pp. 173–204.
Spector,D.L. (1993) *Annu. Rev. Cell Biol.*, **9**, 265–315.
Sugawara,K., Gilead,Z., Wold,W.S.M. and Green,M. (1977) *J. Virol.*, **22**, 527–539.
Tooze,J. (1982) *The Molecular Biology of Tumor Viruses. Volume 2, DNA Tumor Viruses.* 2nd edn, Cold Spring Harbor Laboratory Press, Cold Spring Harbor, NY.
VanDriel,R., Humbel,B. and Jong,L. (1991) *J. Cell. Biochem.*, **47**, 311–316.
Voelkerding,K. and Klessig,D.F. (1986) *J. Virol.*, **60**, 353–362.
Walton,T.H., Moen,Jr, P.,T., Fox,E. and Bodnar,J.W. (1989) *J. Virol.*, **63**, 3651–3660.
Wansink,D.G., Schul,W., van der Kraan,I., van Steensel,B., van Driel,R. and de Jong,L. (1993) *J. Cell Biol.*, **122**, 283–293.
Wansink,D.G., Manders,E.E.M., van der Kraan,I., Aten,J.A., van Driel,R. and de Jong,L. (1994) *J. Cell Sci.*, **107**, 1449–1456.
Wolgemuth,D.J. and Hsu,M.T. (1981) *J. Mol. Biol.*, **147**, 247–268.
Xing,Y., C.,V. Johnson, Dobner,P.R. and Lawrence,J.B. (1993) *Science*, **259**, 1326–1330.
Ziff,E.B. (1980) *Nature*, **287**, 491–499.

Received on May 30, 1994; revised on July 20, 1994